Optical absorption in a two-dimensional quantum point contact

Anna Grincwajg, M. Jonson, and R. I. Shekhter
Department of Applied Physics, Chalmers University of Technology and University of Göteborg, S-412 96 Göteborg, Sweden
(Received 21 September 1993)

We calculate the optical absorption of a quantum point contact. We find that the absorption in the very center of the microconstriction is clearly separated in frequency from the absorption in the wide contact regions. Therefore optical point contact spectroscopy is possible and can be very useful in characterizing the shape of the laterally confining potential. We show how two different types of potentials produce entirely different spectra. Further, optical point contact spectroscopy is found to be sample independent since the microconstriction geometry has practically no influence on the absorption, as long as we consider adiabatic geometries.

I. INTRODUCTION

Ballistic transport in two-dimensional electron systems has attracted a lot of attention during recent years. The possibility of fabricating structures of dimensions comparable to the Fermi wavelength and smaller than the mean free path naturally opens up exciting possibilities for both experimentalists and theoreticians. Among all kinds of structures produced so far, the quantum point contact (QPC) exhibits in a most pure and clear way the principal phenomena in ballistic transport.[1]

The QPC is created by putting a split gate on top of a GaAs heterostructure, thereby causing a depletion layer in the two-dimensional electron gas (2DEG). Two almost separate regions of 2DEG are formed, joined by a "point contact" whose width is controlled by the gate voltage. Since the electrons move through the point contact without suffering any collisions, their motion is analogous to the propagation of an electromagnetic field through a waveguide. The width of the "waveguide" is of the same order as the Fermi wavelength and governs the number of propagating modes.

Several features of the quantum point contact, like quantized conductance and the performance in a magnetic field, have been thoroughly investigated both experimentally[2–4] and theoretically.[5,6] The optical properties, however, have to our knowledge not been the subject of investigations. In this work we calculate the optical absorption spectrum of a QPC. We show that optical point contact spectroscopy (OPCS) certainly is possible and that it can be very useful in characterizing the shape of the laterally confining potential. The shape of this potential is still an open question.

The absorption of a high-frequency field in a quantum point contact is due to electron transitions between different modes, or, in other words, transverse energy states in the system. The transition frequency ω between the modes n and $n+1$ is related to the difference in transverse energy and for a laterally confining potential of the "hard wall" type we have

$$\omega(x) = \frac{\hbar}{2m^*}\frac{\pi^2(2n+1)}{d^2(x)}, \tag{1}$$

where m^* is the electron effective mass and $d(x)$ is the width of the microconstriction (see Fig. 1). Since the transition frequency ω is x dependent, it is not at first sight obvious that the spectrum contains any distinct features. Contributions from transitions in all parts of the microconstriction, including the wide contact regions, must be added, seemingly resulting in a continuous absorption spectrum. However, as we will show, the states in the center of the point contact cause very distinct high-frequency peaks, while the bulk states give a low-frequency contribution to the spectrum.[7] This clear frequency separation is due to a drastic increase of absorption as the frequency reaches its maximum value

$$\omega_{\max} = \frac{\hbar}{2m^*}\frac{\pi^2(2n+1)}{d^2(0)}, \tag{2}$$

corresponding to transitions in the very center of the microconstriction. Qualitatively it can be explained as follows. Consider the interval $[x, x+\Delta x]$ connected to absorption in the frequency range $[\omega, \omega+\Delta\omega]$. The region Δx can, by expanding ω around x, be expressed as

$$\frac{\Delta x}{l} \sim \begin{cases} \frac{l\Delta\omega}{x\omega} & \text{if } \frac{x}{l} > \sqrt{\frac{\Delta\omega}{\omega}}, \\ \sqrt{\frac{\Delta\omega}{\omega}} & \text{if } \frac{x}{l} < \sqrt{\frac{\Delta\omega}{\omega}}, \end{cases} \tag{3}$$

where l is the effective length of the microconstriction (see below). As $x \to 0$ the absorption region Δx increases, to reach its saturation value at $x = 0$ corresponding to $\omega = \omega_{\max}$. Therefore the absorption spectrum will

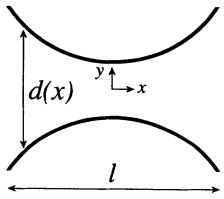

FIG. 1. Geometry of the quantum point contact. The width is denoted by $d(x)$ and the effective length (see text) is denoted by l.

0163-1829/94/49(11)/7557(7)/$06.00

have a peak at $\omega = \omega_{\max}$. We stress that it is the transport electrons, i.e., the propagating modes, that are responsible for the high-frequency peaks, since they are the only ones able to reach the center of the microconstriction. Thus it is the mechanism of frequency separation between bulk and transport electrons that makes optical point contact spectroscopy possible and higly effective.

One interesting application of OPCS is characterization of the laterally confining potential. Because of the transverse energy quantization, different potentials produce different spectra. We compare two types; the square ("hard wall") potential and the parabolic ("soft wall") potential. For a square potential the maximum frequency $\omega_{\max}$ is given by Eq. (2) (taking into account only nearest-mode transitions). The resulting high-frequency spectrum is then consequently a series of equally spaced peaks, each peak corresponding to a propagating mode. In the case of a parabolic potential the maximum frequency is

$$\omega_{\max} = \frac{\hbar}{2m^*}\frac{2}{d^2(0)}, \tag{4}$$

which is independent of n, since the energy levels are equidistant. Therefore all transitions between the propagating modes n and $n+1$ are peaked at the same frequency (only nearest-mode transitions are allowed in this case) and the spectrum contains only one high-frequency peak. Thus we find a characteristic difference between these two spectra, which opens up possibilities of distinguishing experimentally between different types of potentials.

We have also investigated the influence of different microconstriction geometries on the absorption. The sensitivity to geometry was found to be very small, and therefore we conclude that optical point contact spectroscopy is sample independent.

In Sec. II we give a detailed formulation of the problem and derive the basic expressions needed to calculate the optical absorption. In Sec. III we calculate the absorption for different laterally confining potentials and microconstriction geometries. Finally, our results are presented and discussed in Sec. IV, where we also estimate the possibility of experimental realization of OPCS.

II. FORMULATION OF THE PROBLEM

One possible realization of an experiment measuring the optical absorption is to place the QPC in a microwave resonator of size L. In this case the absorption in the QPC will result in a special frequency dependence of the quality factor (Q factor) of the system. Absorption results in dissipation of the electromagnetic field and its strength can be characterized by an absorption coeficient

$$\gamma = \frac{1}{W}\frac{dW}{dt}. \tag{5}$$

Here W is the energy of the electromagnetic field in the resonator. We can treat the field as N coherent photons occupying the single photonic state characterized by the polarization $\hat{\epsilon}$ and frequency ω:

$$W = N\hbar\omega, \quad N = \langle a^\dagger a\rangle. \tag{6}$$

The operators $a^\dagger$ and a are creation and annihilation operators in this photonic state.

Our aim is to calculate the absorption coefficient γ, which according to (5) and (6) can be expressed as

$$\gamma = -\frac{i}{N\hbar}\langle[a^\dagger a, H]\rangle. \tag{7}$$

Here the brackets imply quantum mechanical as well as thermodynamic averaging over all electronic and photonic degrees of freedom.

We consider the Hamiltonian of our system to be a sum of three parts:

$$H_{\rm tot} = H_{\rm electron} + H_{\rm photon} + H_{\rm int}, \tag{8}$$

$$H_{\rm el} = \sum_\alpha E_\alpha c_\alpha^\dagger c_\alpha, \tag{9}$$

$$H_{\rm ph} = \hbar\omega a^\dagger a. \tag{10}$$

Here $c_\alpha^\dagger$ and c_α are creation and annihilation operators for electrons in state α. Keeping only the dipole term of the electron-photon interaction[8] we have

$$H_{\rm int} = \sum_{\alpha\beta}\{A_{\alpha\beta}c_\alpha^\dagger c_\beta + \text{H.c.}\}(a + a^\dagger), \tag{11}$$

with the matrix element $A_{\alpha\beta}$ of the form

$$A_{\alpha\beta} = -\frac{e}{2m^*}\left(\frac{2\pi}{L^3 w}\right)^{1/2}\langle\alpha|p\cdot\hat{\epsilon}|\beta\rangle, \tag{12}$$

where p is the electron momentum operator.

Taking the electromagnetic field in the quasiclassical approximation ($N \gg 1$) we can easily get the absorption coefficient in second-order perturbation theory in the electron-photon coupling as

$$\gamma = \frac{8\pi}{\hbar}\sum_{\alpha\beta}\delta(E_\alpha - E_\beta + \hbar\omega)|A_{\alpha\beta}|^2(n_\beta - n_\alpha). \tag{13}$$

Here n_α and n_β denote the number of electrons in state α and β respectively. In the following section we will explicitly calculate the matrix element $A_{\alpha\beta}$ and the absorption coefficient γ for different laterally confining potentials and microconstriction geometries.

III. CALCULATION OF THE ABSORPTION

The electronic state $|\alpha\rangle$ can be characterized by three quantum numbers as follows

$$|\alpha\rangle = |n, E, \sigma\rangle, \quad n = 1, 2, 3..., \quad \sigma = \pm 1. \tag{14}$$

Here n is the mode number, E is the total energy of the electron, and σ specifies whether the electron moves in the positive or negative x direction. In the case of an adiabatic geometry, the electron wave function of mode n

can be separated into one longitudinal and one transverse part:[5]

$$\Xi_n(x,y) = \Psi_n(x)\Phi_{n,x}(y) . \tag{15}$$

The variable x then appears as a parameter in the transverse wave function $\Phi_{n,x}(y)$.

We will consider the case when the electromagnetic field is polarized in the y direction. In this case the matrix element in Eq. (12) can be expressed as

$$\langle\alpha|p_y|\beta\rangle = -i\hbar \int_{-L/2}^{L/2} dx \Psi_n^*(x)\Psi_m(x) \times \int_{-\infty}^{\infty} dy \Phi_{n,x}^*(y)\frac{\partial}{\partial y}\Phi_{m,x}(y). \tag{16}$$

The transverse wave function depends on the shape of the laterally confining potential. In order to investigate the role of the confining potential forming the QPC, we will consider two different model potentials; a square ("hard wall") potential and a parabolic ("soft wall") potential.

For a square potential, the Schrödinger equation for $\Phi_{n,x}(y)$,

$$-\frac{\hbar^2}{2m^*}\frac{d^2}{dy^2}\Phi_{n,x}(y) = E_n\Phi_{n,x}(y), \tag{17}$$

$$\Phi_{n,x}\left(y = \pm\frac{d(x)}{2}\right) = 0, \tag{18}$$

has the solution

$$\Phi_{n,x}(y) = \sqrt{\frac{2}{d(x)}}\sin\left[\frac{n\pi}{d(x)}\left(y + \frac{d(x)}{2}\right)\right], \tag{19}$$

which gives the transverse energy

$$E_n = \frac{\hbar^2}{2m^*}\frac{n^2\pi^2}{d^2(x)}. \tag{20}$$

The y integral in the matrix element can now be evaluated:

$$\int_{-d(x)/2}^{d(x)/2} dy \Phi_{n,x}(y)\frac{d}{dy}\Phi_{m,x}(y) = \frac{4}{d(x)}\frac{nm}{n^2-m^2}\delta_{n+m,\text{odd}} . \tag{21}$$

For a parabolic potential,[9] the Schrödinger equation for $\Phi_{n,x}(y)$,

$$-\frac{\hbar^2}{2m^*}\left[\frac{d^2}{dy^2} - \frac{y^2}{d^4(x)}\right]\Phi_{n,x}(y) = E_n\Phi_{n,x}(y), \tag{22}$$

has the following solution, expressed in terms of the dimensionless variable $\xi = y/d(x)$:

$$\Phi_{n,x}(\xi) = A_n H_n(\xi)e^{-\xi^2/2}, \tag{23}$$

$$A_n = (2^n n!)^{-1/2}\left(\frac{1}{\pi d^2(x)}\right)^{1/4},$$

where $H_n(\xi)$ is the Hermite polynomial of order n and A_n is a normalization constant. The resulting transverse energy

$$E_n = \frac{\hbar^2}{2m^*}\frac{2n+1}{d^2(x)}, \tag{24}$$

has the well-known harmonic oscillator dependence. The y integral in the matrix element is evaluated as

$$\int_{-\infty}^{\infty} dy \Phi_{n,x}(y)\frac{d}{dy}\Phi_{m,x}(y) = \frac{1}{\sqrt{2}d(x)}\left\{\sqrt{n+1}\delta_{m,n+1} - \sqrt{n}\delta_{m,n-1}\right\}. \tag{25}$$

Now we can evaluate the x integral in the matrix element. Since the x dependence of the two expressions (21) and (25) is identical, the x integral will be the same for both potentials. The expression for the longitudinal wave function $\Psi_n(x)$ depends on whether the mode n is propagating or not:

$$\Psi_n(x) = \begin{cases} \frac{1}{\sqrt{L}}\exp[i\sigma\int^x dx' k_n(x')] & \text{if } E - E_n(0) > 0 , \\ \sqrt{\frac{2}{L}}\sin[\int_{x_n}^x dx' k_n(x')] & \text{if } E - E_n(0) < 0 . \end{cases} \tag{26}$$

The first expression is for propagating modes; the normalization length L is the length of the resonator, $k_n(x)$ is the longitudinal wave vector of mode n, and x_n is the turning point for the nonpropagating mode. Assuming that n and m are transport modes we have

$$\int_{-L/2}^{L/2}\frac{dx}{d(x)}\Psi_n^*(x)\Psi_m(x) = \frac{1}{L}\int_{-L/2}^{L/2}\frac{dx}{d(x)} \times \exp[-i\sigma\alpha_n(x) + i\sigma'\alpha_m(x)], \tag{27}$$

where

$$\alpha_n(x) = \int^x k_n(x')dx', \tag{28}$$

$$\alpha_m(x) = \int^x k_m(x')dx'. \tag{29}$$

Since we are dealing with an adiabatic geometry the phase $\varphi(x) = \sigma\alpha_n(x) - \sigma'\alpha_m(x)$ in the above integral depends almost linearly on x. Let us therefore expand $\varphi(x)$ around the point x^* where the first derivative is zero, which is possible only if $\sigma = \sigma'$:

$$\sigma[\alpha_n(x) - \alpha_m(x)] \approx \sigma\{\alpha_n(x^*) - \alpha_m(x^*) + \tfrac{1}{2}(x - x^*)^2[\alpha_n''(x^*) - \alpha_m''(x^*)]\}. \tag{30}$$

The requirement that the first derivative shall be zero at $x = x^*$ implies that

$$k_n(x^*) = k_m(x^*). \tag{31}$$

We can now evaluate the integral using the fact that

$d(x)$ varies slowly compared to the rapidly oscillating exponential function. Making the approximation $d(x) = d(x^*)$ and using the above expansion we get

$$\int_{-L/2}^{L/2} \frac{dx}{d(x)} \Psi_n^*(x)\Psi_m(x) = \frac{2\pi}{Ld(x^*)} \frac{e^{-i\varphi(x^*)}\delta_{\sigma,\sigma'}}{\sqrt{|k_n'(x^*) - k_m'(x^*)|}}. \tag{32}$$

The energy conservation law $E_\beta = E_\alpha + \hbar\omega$ [see Eq. (13)] implies that the longitudinal wave vectors can be expressed in terms of the total energy E of the initial state and the frequency ω as

$$k_n(x) = \sqrt{\frac{2m^*}{\hbar^2}[E - E_n(x)]} \tag{33}$$

$$k_m(x) = \sqrt{\frac{2m^*}{\hbar^2}[E + \hbar\omega - E_m(x)]}. \tag{34}$$

Here the transverse energies for the two different potentials are given by Eqs. (20) and (24). From this we get

$$|k_n'(x^*) - k_m'(x^*)| = \frac{2m^*}{\hbar^2 k_n(x^*)} \left|\frac{d'(x^*)}{d(x^*)}\right| \times [E_m(x^*) - E_n(x^*)]. \tag{35}$$

The expression $k_n(x^*) = k_m(x^*)$ can with the use of the energy conservation law be rewritten as

$$\hbar\omega = E_m(x^*) - E_n(x^*). \tag{36}$$

This formula represents the picture of local intermode transitions presented in the introduction. The requirement is that there exists a point x^* that satisfies the above equation which can be expressed as the inequality

$$\hbar\omega < E_m(0) - E_n(0)\ . \tag{37}$$

So far we have assumed that both n and m are propagating modes. However it can easily be shown also that if one or both of them are nonpropagating, the above results will be the same. In the case of one propagating and one nonpropagating mode there will be a difference of a factor 1/2 from the wave-function normalization. But since there will be no restriction $\delta_{\sigma,\sigma'}$ in this case this factor of 1/2 will be canceled by the additional summation over σ. In the case where both modes are nonpropagating the condition $\delta_{\sigma,\sigma'}$ will be imposed trivially. However, the difference in wave-function normalization turns out to be canceled by other factors in the wave function.

The existence of turning points imposes the condition that the point x^* must be in the region allowed for the wave function, or equivalently

$$k_n^2(x^*) \geq 0. \tag{38}$$

Using Eq. (36) we can express $k_n(x^*)$ for the square potential as

$$k_n(x^*) = \sqrt{\frac{2m^*}{\hbar^2}\left(E - \hbar\omega\frac{n^2}{m^2 - n^2}\right)}, \tag{39}$$

and for the parabolic potential

$$k_n(x^*) = \sqrt{\frac{2m^*}{\hbar^2}[E - \hbar\omega(n + \tfrac{1}{2})]}. \tag{40}$$

We are now ready to write down the expression for the absorption coefficient. Because of the energy conservation law only one integration over energy is needed. We include a factor of 2 for spin, put the temperature to zero, and introduce the dimensionless variables $\epsilon = E/E_0$, $\epsilon_F = E_F/E_0$, $\Omega = \hbar\omega/E_0$, and $D = d(0)/d(L/2)$ for, respectively, energy, Fermi energy, frequency, and constriction width. The energies are normalized to

$$E_0 = \frac{\hbar^2}{2m^*}\frac{\pi^2}{d^2(0)}, \tag{41}$$

the lowest transvere energy in a square "hard wall" confining potential of width $d(0)$. Our result in the case of the square potential is

$$\gamma_{\rm sq} = \alpha\frac{c}{L}\frac{d(0)}{L^2}\frac{128}{\pi^2}\sum_{n,m}\delta_{n+m,\rm odd}\frac{n^2m^2}{(m^2-n^2)^3} \times \left|\frac{d(x^*)}{d'(x^*)}\right|\Theta[m^2 - n^2 - \Omega]\int\frac{d\epsilon}{\Omega}\mathcal{F}_{\rm sq}(\epsilon), \tag{42}$$

where $\alpha = e^2/\hbar c$ is the fine-structure constant, c is the velocity of light, and

$$\mathcal{F}_{\rm sq}(\epsilon) = \frac{\Theta[\epsilon - n^2D^2]\Theta[\epsilon + \Omega - m^2D^2]}{\sqrt{\epsilon - n^2D^2}\sqrt{\epsilon + \Omega - m^2D^2}} \times\sqrt{\epsilon - \Omega n^2/(m^2-n^2)} \times\Theta[\epsilon - \Omega n^2/(m^2-n^2)]\Theta[\epsilon_F - \epsilon]\Theta[\epsilon + \Omega - \epsilon_F]\ . \tag{43}$$

In the case of the parabolic potential we have

$$\gamma_{\rm par} = \alpha\frac{c}{L}\frac{d(0)}{L^2}2\pi\sum_n(n+1)\left|\frac{d(x^*)}{d'(x^*)}\right| \times\Theta[2 - \pi^2\Omega]\int\frac{d\epsilon}{\Omega}\mathcal{F}_{\rm par}(\pi^2\epsilon), \tag{44}$$

where

$$\mathcal{F}_{\rm par}(\epsilon) = \frac{\Theta[\epsilon - (2n+1)D^2]\Theta[\epsilon + \pi^2\Omega - (2n+3)D^2]}{\sqrt{\epsilon - (2n+1)D^2}\sqrt{\epsilon + \pi^2\Omega - (2n+3)D^2}} \times\sqrt{\epsilon - \pi^2\Omega(n+1/2)}\Theta[\epsilon - \pi^2\Omega(n+1/2)] \times\Theta[\pi^2\epsilon_F - \epsilon]\Theta[\epsilon + \pi^2(\Omega - \epsilon_F)]\ . \tag{45}$$

The absorption coefficient γ depends on the microconstriction geometry $d(x)$ through the factor $|d(x^*)/d'(x^*)|$. To determine its importance we have calculated γ for two different geometries, one for which the constriction width has an exponential dependence on the x coordinate

$$d(x) = d(0)e^{x^2/2l^2}, \tag{46}$$

and one for which this dependence is quadratic,

$$d(x) = d(0)/[1 + x^2/l^2]. \tag{47}$$

In both cases the length scale of the microconstriction is determined by the parameter l; for the exponential geometry we get

$$\left|\frac{d(x^*)}{d'(x^*)}\right| = \frac{l}{\sqrt{\ln \beta_{mn}^2}}, \tag{48}$$

and for the quadratic geometry

$$\left|\frac{d(x^*)}{d'(x^*)}\right| = \frac{l\beta_{mn}}{2\sqrt{\beta_{mn}-1}}, \tag{49}$$

where

$$\beta_{mn} = \sqrt{\frac{E_m(0)-E_n(0)}{\hbar\omega}}\,. \tag{50}$$

Before we end this section we note that the absorption coefficients $\gamma_{\rm sq}$ and $\gamma_{\rm par}$ [see Eqs. (42),(44) and (48),(49)] are proportional to the fine-structure constant α which characterizes the strength of the coupling between light and matter, to the factor c/L which is the inverse time it takes an electromagnetic wave to propagate through the resonator, and to the factor $ld(0)/L^2$ which is the ratio of the effective point-contact absorption area to the total resonator area.

IV. RESULTS AND DISCUSSION

In this section we will analyze various absorption spectra resulting from our calculations using the following values of parameters entering our expressions: the Fermi wavelength $\lambda_F = 400$ Å, the length scale of the microconstriction $l = 1\mu$m, and the length of the resonator $L = 1$ mm.

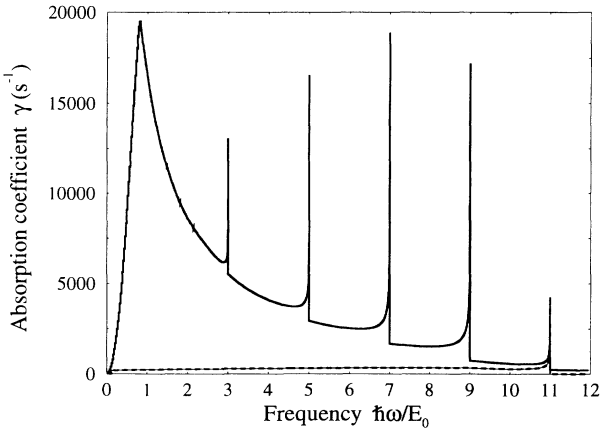

FIG. 2. Frequency dependence of the absorption coefficient of a quantum point contact in the case of a square-type laterally confining potential. In this case there are five transport modes in the channel, resulting in five narrow absorption peaks. The dashed line shows the separate contribution from the fifth transport mod e, which is seen to dominate the contribution to the fifth peak. The wide maximum at low frequencies is a result of absorption in the contact regions (bulk absorption). The energy is normalized to $E_0 = \hbar^2\pi^2/2m^*d^2(0)$ and in this case we have used $d(0) = 1100$ Å.

Figure 2 shows the absorption coefficient γ as a function of frequency for the square potential case. The channel has five propagating modes and consequently we find five absorption peaks, positioned at the frequencies $\omega = (2n+1)E_0/\hbar$. Because of the matrix element the absorption peaks resulting from nearest-mode transitions are considerably larger than those resulting from other transitions. There is therefore no appreciable absorption at frequencies higher than those included in the figures. The microconstriction geometry in this figure is of the exponential type.

It is also seen that the bulk absorption, which is responsible for the wide maximum at low frequencies in Fig. 2, is very well separated from the narrow peaks due to absorption in the center part of the constriction. The bulk absorption results from transitions between nonpropagating modes, i.e., modes whose wave functions have a turning point. Since the nonpropagating modes do not reach the center of the microconstriction, they do not develop any resonant absorption peaks. The dashed line in Fig. 2 shows the contribution from mode $n = 5$ and it is clearly seen that the fifth peak consists entirely of this contribution. We therefore stress again that the bulk absorption does not affect the absorption in the center of the point contact.

It can be seen in the equations that the absorption coefficient γ depends on $d(L/2)$. A natural choice would at first sight be to let $d(L/2) \to \infty$, but this is not possible since our adiabatic model is not valid on length scales exceeding the impurity scattering length. Therefore we have introduced a maximum width of the channel, $d_{\rm max}$, which is not allowed to exceed the inelastic scattering length. In our numerical calculations we have used $d_{\rm max} \approx 10d(0)$, but the value of $d_{\rm max}$ does not have any significant influence on the resonant absorption peaks. However it strongly affects the bulk absorption, a matter we dicuss below.

The magnitude of the bulk absorption grows with increasing $d_{\rm max}$, since it is proportional to the number of modes in the wide regions. It is found that the bulk absorption grows as $d_{\rm max}^{2-\eta}$ where η is a positive number smaller than unity. Hence the absorption *density* goes to zero as $d_{\rm max} \to \infty$, in agreement with the well-known result for bulk materials. Since we are dealing with a finite $d_{\rm max}$ in our calculations, a threshold value of the transition frequency ω enters, below which no absorption can take place. This is seen in Fig. 2, where we also note that the sawtooth structure in the bulk absorption is due to new modes being switched on as the frequency increases.

For transitions at the very center of the microconstriction, $x = 0$, the denominator $d'(x^*)$ is zero and hence the absorption coefficient γ becomes infinite in our simple model. To avoid this divergence we have added a small number δ to the denominator.

The dependence of the absorption on microconstriction geometry is found to be very weak, a fact which indicates that OPCS should be sample independent. Figure 3 shows a comparison of the absorption coefficients for two different geometries. The solid line represents the exponential geometry and the dashed line represents the quadratic case. The laterally confining potential is of the

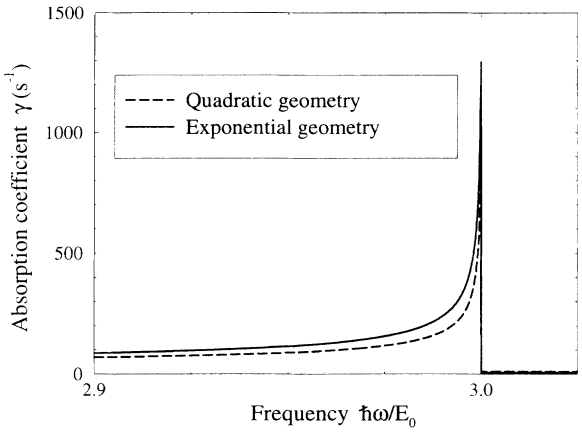

FIG. 3. Absorption coefficient as a function of frequency for two different microconstriction geometries. The solid line corresponds to the exponential geometry and the dashed line corresponds to the quadratic geometry (see text). It is seen that the difference between them is very small, a fact indicating that optical point contact spectroscopy should be sample independent. There is one transport mode in the system and the laterally confining potential is of the square type for both geometries. The energy is normalized to $E_0 = \hbar^2\pi^2/2m^*d^2(0)$ and in this case we have $d(0) = 300$ Å.

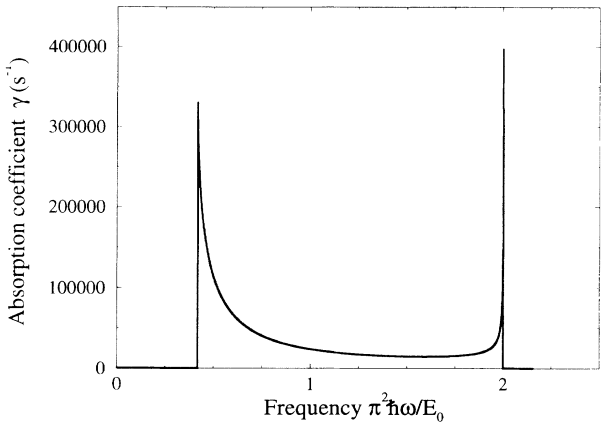

FIG. 4. Frequency dependence of the absorption coefficient in the case of a parabolic-type laterally confining potential. There are twelve transport modes in the channel, together resulting in a single absorption peak. The wide maximun at low frequencies is a result of absorption in the contact regions (bulk absorption). The energy is normalized to $E_0 = \hbar^2\pi^2/2m^*d^2(0)$ and in this case we have $d(0) = 320$ Å.

square type, and we have one propagating mode in the system. The difference between the two types of geometry is seen to be very small, and the same result is found for the parabolic potential.

Now let us turn our attention to the case of the parabolic potential. Since the energy levels are equidistant in a parabolic potential, all transitions between the propagating modes n and $n+1$ are peaked at the same frequency. (For this type of potential only nearest-mode transitions are allowed, i.e., $m = n + 1$.) Figure 4 shows the absorption coefficient γ as a function of frequency for a channel with twelve propagating modes. We see that there is only one absorption peak, positioned at the frequency $\omega = 2\pi^2 E_0/\hbar$. The bulk absorption, which also here is very well separated from the absorption peak, has the same properties as in the case of the square potential discussed above.

We will now estimate the possibilities of an experimental realization of optical point contact spectroscopy. We imagine that the point contact device should be put into an electromagnetic resonator, which can be characterized by a quality factor q_0 defined as

$$q_0 = \frac{\omega}{\gamma_0}, \tag{51}$$

where γ_0 is the absorption coefficient of the resonator. In analogy we can define a quality factor of the point contact as

$$q_{PC} = \frac{\omega}{\gamma_{PC}} \tag{52}$$

where γ_{PC} is the absorption coefficient of the point contact. The entire system when the point contact is put inside the resonator can then be characterized by the total quality factor

$$Q = \frac{q_0}{1 + q_0/q_{PC}} \tag{53}$$

We assume that the ratio q_0/q_{PC} must be at least as large as 1/10, to make the point contact absorption measurable. The quality factor for the resonator is taken to be[10] $q_0 = 10^8$. The smallest q_{PC} values are found for the parabolic potential case. For a point contact with five propagating modes we get $q_{PC} \approx 8 \times 10^8$ and for twelve propagating modes we get $q_{PC} \approx 0.5 \times 10^8$. This gives us $q_0/q_{PC} = 1/8$ and $q_0/q_{PC} = 2$, respectively. In the square potential case we get for five propagating modes $q_{PC} \approx 2 \times 10^9$ and for ten propagating modes $q_{PC} \approx 2 \times 10^8$. This gives $q_0/q_{PC} = 1/20$ and $q_0/q_{PC} = 1/2$, respectively. Our crude estimate indicates that point contact absorption can be measured if the number of propagating modes is large. Especially if the laterally confining potential is of the parabolic type, the conditions for an experimental realization seem to be good.

In conclusion we have calculated the optical absorption of a quantum point contact. We have found that the absorption in the very center of the microconstriction is clearly separated in frequency from the absorption in the wide contact regions. Therefore optical point contact spectroscopy is possible and can be very useful in characterizing the shape of the laterally confining potential. We have shown how two different types of potentials pro-

duce entirely different spectra. Further, OPCS is found to be sample independent since the microconstriction geometry has practically no influence on the absorption, as long as we consider adiabatic geometries. We have also made an estimation of the experimental possibilities of measuring point contact absorption.

ACKNOWLEDGMENTS

This work was supported by the Swedish Natural Science Research Council and by NUTEK. It is a pleasure to acknowledge useful discussions with S. Andersson, J. Carini, and D. K. Ferry.

[1] C. W. J. Beenakker and H. van Houten, in *Solid State Physics: Advances in Research and Applications*, edited by H. Ehrenreich and D. Turnbull (Academic, San Diego, 1991), Vol. 44, p. 1.

[2] B. J. van Wees, H. van Houten, C. W. J. Beenakker, J. G. Williamson, L. P. Kouwenhoven, D. van der Mare, and C. T. Foxon, Phys. Rev. Lett. **60**, 848 (1988).

[3] D. A. Wharam, T. J. Thornton, R. Newbury, M. Pepper, H. Ahmed, J. E. F. Frost, D. G. Hasko, D. C. Peacock, D. A. Ritchie, and G. A. C. Jones, J. Phys. C **21**, L209 (1988).

[4] B. J. van Wees, L. P. Kouwenhoven, H. van Houten, C. W. J. Beenakker, J. E. Mooji, C. T. Foxon, and J. J. Harris, Phys. Rev. B **38**, 3625 (1988).

[5] L. I. Glazman, G. B. Lesovik, D. E. Khmelnitskii, and R. I. Shekhter, Pis'ma Zh. Eksp. Teor. Fiz. **48**, 329 (1988) [JETP Lett. **48**, 238 (1988)].

[6] L. I. Glazman and M. Jonson, Phys. Rev. B **41**, 10 686 (1990).

[7] This is true for any shape of the laterally confining potential, as long as the length of the adiabatic QPC is much larger than the Fermi wavelength.

[8] A. Messiah, *Quantum Mechanics* (North-Holland, Amsterdam, 1970), Chap. 21, p. 1037.

[9] M. Büttiker, Phys. Rev. B **41**, 7906 (1990).

[10] This value of q_0 is a reasonable estimate for a high-quality microwave dielectric resonator at cryogenic temperatures; J. Carini (private communication).